
Matryoshka Concept Bottleneck Models

Ziye Chen¹, Hongbin Lin¹, Xinyue Xu², Jie Li³, Lijie Hu⁴

¹The Hong Kong University of Science and Technology (Guangzhou)

²The Hong Kong University of Science and Technology

³China University of Petroleum-Beijing at Karamay

⁴Mohamed bin Zayed University of Artificial Intelligence

Abstract

Concept Bottleneck Models (CBMs) have emerged as a prominent paradigm for interpretable deep learning, learning by grounding predictions in human-understandable concepts. However, their practical deployment is hindered by the high cost of test-time intervention, as correcting model errors typically requires human experts to manually inspect and verify a large set of predicted concepts. Existing approaches suffer from a fundamental structural limitation: they either adopt a single static concept set, forcing experts to exhaustively annotate concepts and incurring prohibitive intervention costs, or train multiple models tailored to different concept budgets, resulting in substantial computational and maintenance overhead. To address this challenge, we propose the **Matryoshka Concept Bottleneck Model (MCBM)**, a unified architecture that enables adaptive concept utilization within a single model. Inspired by Matryoshka Representation Learning, MCBM organizes concepts into a nested hierarchy based on maximum relevance and minimum redundancy, allowing inference at multiple levels of conceptual granularity without retraining. Theoretically, we show that MCBM reduces the expected intervention costs from linear to logarithmic order, $O(\log K)$, while guaranteeing monotonic performance improvement. Empirically, extensive experiments demonstrate that MCBM matches the performance of independently trained models while enabling dynamic and efficient expert interaction.

1 Introduction

As deep learning models are increasingly deployed in high-stakes domains such as healthcare and finance, transparency and interpretability have become central concerns [14, 10]. Concept Bottleneck Models (CBMs) [11] address this challenge by decomposing predictions into two interpretable stages: mapping inputs to human-understandable concepts and making predictions solely based on these concepts. Beyond providing explanations, CBMs enable human experts to intervene by inspecting and correcting erroneous concept predictions, motivating growing interest in effective and interactive CBM design [24].

However, the practical utility of CBMs is hindered by the high cost of test-time intervention. Existing CBM approaches treat concepts as a flat and unordered set, requiring experts to manually inspect and correct many concepts to fix a single prediction [4], rendering large-scale deployment impractical. While reducing the number of concepts can lower this burden, it often leads to a substantial drop in predictive performance [9]. As a result, practitioners face a rigid design choice: either deploy a single high-dimensional CBM that is costly to intervene on, or train and maintain multiple models with different concept budgets, incurring significant computational overhead and lacking flexibility for real-world deployment.

This rigidity arises from how concepts are structured and utilized in existing CBMs. In fine-grained tasks, many concepts are redundant, yet standard CBM approaches treat them as independent and equally important, leading to inefficient intervention. A natural solution is to exploit the information-

theoretic structure of concept sets. Organizing concepts into a nested hierarchy based on **Maximum Relevance and Minimum Redundancy (mRMR)** concentrates discriminative information in early concept dimensions. This organization aligns with Matryoshka Representation Learning, where representations are ordered by decreasing importance within a single model, offering a principled route to efficient and adaptive intervention.

To operationalize this insight, we introduce the **Matryoshka Concept Bottleneck Model (MCBM)**. As illustrated in Figure 1, MCBM is a unified architecture designed for flexible and cost-efficient deployment. Unlike existing methods that require training separate models for different concept budgets, our framework is trained once and supports adaptive inference across a wide range of intervention constraints. Specifically, we employ the mRMR criterion to construct a hierarchical ordering of concepts, ensuring that the most informative and least redundant concepts are prioritized. The model is then optimized using a nested objective function that enforces predictive accuracy at multiple levels of conceptual granularity simultaneously. Consequently, MCBM functions as a plug-and-play module, allowing practitioners to dynamically trade off annotation cost and predictive performance without retraining.

Our main contributions are summarized as follows:

- **Methodology:** We introduce MCBM, a unified architecture that integrates mRMR-based concept ordering with Matryoshka Representation Learning, enabling elastic deployment and efficient intervention from a single training run.
- **Theoretical Analysis:** We show that the proposed nested, importance-based structure reduces the expected intervention cost from linear $O(K)$ to logarithmic $O(\log K)$ under standard information decay assumptions.
- **Experiments:** We empirically validate MCBM on the CUB, LAD, and CelebA datasets, demonstrating performance comparable to independently trained baselines with substantially reduced intervention effort.

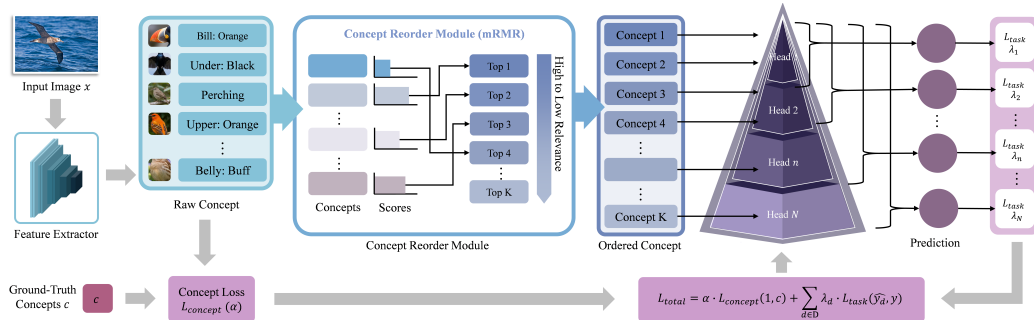


Figure 1: **Matryoshka Concept Bottleneck Models Architecture.** The input image is encoded into raw logits, which are then permuted based on the pre-computed mRMR ranking. This yields an ordered concept vector where information density is concentrated at the beginning. Multiple parallel heads (Matryoshka Heads) then perform classification using nested prefixes of this ordered vector.

2 Related Work

Concept Bottleneck Models and the Rigid Cost Paradigm. Concept Bottleneck Models (CBM) [11] have established themselves as a cornerstone of interpretable deep learning, particularly in high-stakes domains like healthcare [1, 26] and dermatology [6], where distinguishing specific attributes is critical for trust. The core appeal of CBM lies in their ability to support test-time intervention [20], allowing human experts to rectify mispredictions. Recent work improves CBM along orthogonal axes such as robustness, label-efficiency, faithfulness, and concept-set completeness [9, 16, 27, 28, 13, 3]. However, despite these advances in model quality, existing approaches fundamentally neglect the *inference efficiency* of the bottleneck itself. Whether supervised or label-free [16, 25], these models structure concepts as a *flat, unordered bottleneck*, imposing a rigid $O(K)$ verification cost on the user regardless of the input’s difficulty. Our Matryoshka CBM

(MCBM) addresses this overlooked dimension by introducing a nested hierarchy, enabling efficient, logarithmic-cost interventions without sacrificing the robustness or faithfulness gains of prior arts.

Sparse, Hybrid, and Adaptive CBM. To mitigate the computational and cognitive overhead of CBM, a second line of work introduces sparsity or hybrid mechanisms. *Hybrid CBM* combine concept bottlenecks with standard black-box branches to recover performance [2, 9], but often at the cost of full interpretability. *Sparse CBM* utilize regularization techniques (e.g., L_1 penalties, Gumbel-Softmax) to dynamically select a small subset of active concepts per input [19, 23]. Similarly, *Adaptive CBM* attempt to adjust the bottleneck capacity to handle distribution shifts [5]. However, these methods typically result in *unstructured sparsity* where the model activates a disparate set of concepts for each individual sample. This lack of a globally consistent ordering prevents systematic resource truncation (e.g., for deployment on edge devices with fixed memory budgets). Furthermore, they lack a theoretical guarantee for intervention efficiency. In contrast, MCBM enforces a *globally consistent, importance-based ordering* via mRMR, enabling predictable plug-and-play deployment and theoretically bounded intervention costs.

Causal and Stochastic CBM. Causal and stochastic CBMs model dependencies among concepts to improve intervention propagation and uncertainty-aware reasoning [21, 7]. This direction is complementary to ours. Such models answer how a correction should propagate through a concept graph, while MCBM answers which concepts should be queried first under a strict human or hardware budget. Even when a causal graph identifies task-relevant parents, it does not by itself solve the redundancy-aware subset-ordering problem; highly correlated parents can waste a small intervention budget. Moreover, graph-based propagation usually requires the full concept graph and full vocabulary to remain active at inference time. MCBM instead bakes a static mRMR ordering into the architecture, allowing unused suffix concepts and their heads to be physically truncated for predictable low-resource deployment.

Matryoshka Representation Learning and Feature Selection. Beyond CBM, *Matryoshka Representation Learning (MRL)* [12] enforces nested embeddings for multi-granular inference, while Minimum Redundancy Maximum Relevance (mRMR) [18, 8] orders features to maximize information density. However, MRL operates on opaque latent embeddings unsuitable for human intervention, and mRMR is traditionally limited to tabular data. We unify MRL’s structural efficiency with mRMR’s information-theoretic rigor inside a semantic CBM, yielding a model that is simultaneously interpretable, intervention-efficient, and structurally elastic.

3 Matryoshka Concept Bottleneck Models

In interpretable deep learning, a fundamental tension exists between *model transparency* and *deployment efficiency*. Since runtime concept annotation is costly, standard Concept Bottleneck Models (CBM) face a rigid dilemma: utilizing all concepts incurs prohibitive intervention costs, while discarding them degrades performance. Furthermore, adapting to different resource budgets typically requires training multiple specialized models, creating significant computational overhead.

We introduce the Matryoshka Concept Bottleneck Models (MCBM), which reimagine the concept layer as a *nested information hierarchy* ordered by global importance. A single unified model then supports inference at varying granularities (e.g., top-8, top-16, or all concepts) without retraining, decoupling training from deployment constraints.

3.1 Architecture Overview

The MCBM data flow during end-to-end training follows a three-step pipeline: (1) **Concept Ranking**, which discovers a global topological ordering of concepts; (2) **Matryoshka Encoding**, which projects visual features into this ordered semantic space; and (3) **Nested Prediction**, where parallel heads jointly optimize accuracy across varying concept budgets.

3.1.1 Concept Importance Ranking via mRMR

Intuition. Before training, we fix a hierarchical ordering of all concepts. Ranking concepts by individual discriminative power is insufficient: in fine-grained datasets, top-scoring concepts are

often highly correlated (e.g., “has wings” and “flight capable”), so a naively ranked prefix carries overlapping information and wastes the limited capacity of low-dimensional bottlenecks. We therefore seek a permutation that maximizes the *information density* of every prefix.

Formulation. We employ the Minimum Redundancy Maximum Relevance (mRMR) criterion, a greedy procedure that iteratively picks the concept maximizing relevance to the target while minimizing redundancy with the already selected set. Let Ω be all concepts and \mathcal{S}_{t-1} the $t-1$ already chosen; the t -th concept is selected from $\Omega \setminus \mathcal{S}_{t-1}$ as:

$$c_t = \operatorname{argmax}_{c_i \in \Omega \setminus \mathcal{S}_{t-1}} \left(\underbrace{I(c_i; y)}_{\text{Relevance}} - \frac{1}{|\mathcal{S}_{t-1}|} \sum_{c_j \in \mathcal{S}_{t-1}} \underbrace{I(c_i; c_j)}_{\text{Redundancy}} \right) \quad (1)$$

where $I(\cdot; \cdot)$ denotes the Mutual Information (MI). For discrete variables (binary concepts and categorical labels), MI is defined as:

$$I(X; Y) = \sum_{x \in X} \sum_{y \in Y} P(x, y) \log \frac{P(x, y)}{P(x)P(y)} \quad (2)$$

where $P(x, y)$ is the joint probability distribution and $P(x), P(y)$ are the marginals.

Interpretation. The mRMR score explicitly balances two competing objectives to ensure information efficiency:

- **Max-Relevance** ($I(c_i; y)$): Prioritizes concepts that maximize the mutual information with the target label y , ensuring high predictive power.
- **Min-Redundancy** ($I(c_i; c_j)$): Penalizes candidate concepts that share high mutual information with the already selected set \mathcal{S}_{t-1} , preventing information duplication.

Subtracting the redundancy term acts as a regularizer that favors *complementary* concepts over discriminative but repetitive ones, and using mutual information instead of linear correlation captures non-linear semantic dependencies. The selection runs once *before* network training at negligible $O(K^2)$ cost, producing a fixed topological blueprint that forces the model to populate the most critical semantic channels first.

Intuitive Example. For bird classification, “has red breast” and “has red chest” are both relevant for a Robin but nearly redundant. After selecting “has red breast”, mRMR drops the marginal gain of “has red chest” and instead picks, e.g., “beak shape”, so the first two dimensions cover diverse attributes (color *and* shape) and maximize accuracy of the low-dimensional Matryoshka heads.

3.1.2 Matryoshka Architecture and Joint Optimization

Intuition. Building upon the mRMR-optimized hierarchy, we design the neural architecture to enforce the “Matryoshka property”: the representation at dimension d should be a sufficient statistic for the task, even if dimensions $d+1 \dots K$ are truncated. This implies that the model cannot distribute information arbitrarily; it must compress the most vital semantic signals into the earliest slots defined by our ranking.

Forward Pass and Heads. An input image \mathbf{x} is mapped by a feature extractor $g_\theta(\cdot)$ to a raw concept-logit vector $\mathbf{l} \in \mathbb{R}^K$, then permuted by a deterministic module Π following the mRMR indices into the ordered vector $\mathbf{c}_{\text{ord}} = \Pi(\mathbf{l})$. A set of parallel lightweight heads $\{f_{\phi_d}\}_{d \in \mathcal{D}}$, with nesting granularities $\mathcal{D} = \{d_1, \dots, d_n\}$ (e.g., $\{8, 16, 32, \dots\}$), each act as a linear classifier on the corresponding prefix:

$$\hat{y}_d = f_{\phi_d}(\mathbf{c}_{\text{ord}}[1 : d]) = \mathbf{W}_d \cdot \mathbf{c}_{\text{ord}}[1 : d] + \mathbf{b}_d \quad (3)$$

Because the input is ordered by mRMR, the head f_{ϕ_d} effectively utilizes the maximum possible information encodable in d bits.

Joint Optimization Objective. A joint loss trains the backbone and all heads simultaneously, combining concept alignment with multi-granularity task performance:

$$\mathcal{L}_{\text{total}} = \alpha \cdot \mathcal{L}_{\text{concept}}(\mathbf{l}, \mathbf{c}_{GT}) + \sum_{d \in \mathcal{D}} \lambda_d \cdot \mathcal{L}_{\text{task}}(\hat{y}_d, y_{GT}) \quad (4)$$

In the standard MCBM, the encoder, permutation module, and all prediction heads are optimized in a single end-to-end run under Eq. (3). Each mini-batch supplies concept supervision to preserve human semantics while every head imposes task supervision at its own prefix length, so the model learns one ordered bottleneck whose early coordinates remain useful for every downstream head, rather than stitching together isolated CBMs.

Interpretation of the Loss Dynamics. The first component, **Concept Grounding** ($\mathcal{L}_{\text{concept}}$), is a binary cross-entropy loss against the ground-truth concepts \mathbf{c}_{GT} . It anchors the bottleneck to human-defined semantics; without it, the encoder may treat the bottleneck as arbitrary latent variables and lose interpretability.

The second component, **Nested Task Supervision** ($\sum \mathcal{L}_{\text{task}}$), is the engine of Matryoshka learning. Gradients from every head f_{ϕ_d} backpropagate to the shared encoder, so the earliest dimensions of \mathbf{c}_{ord} accumulate updates from *all* heads in \mathcal{D} while later dimensions receive gradients only from the largest head. This differential pressure forms a “gravity well” that pushes the most robust, generalizable features into the early dimensions, since they must serve every head simultaneously.

3.2 Efficient MCBM: Trading Performance for Memory

Intuition. Standard MCBM uses distinct weights \mathbf{W}_d per nesting level, allowing each head to specialize but incurring a memory cost linear in $|\mathcal{D}|$ and limiting inference to predefined checkpoints. Under tight memory budgets or “any-time” inference (stopping at *any* integer k), this becomes wasteful, motivating the **Efficient MCBM** variant.

Mechanism. Instead of instantiating independent physical heads $\{f_{\phi_d}\}$, the Efficient MCBM utilizes a *single, shared weight matrix* $\mathbf{W}_{\text{shared}} \in \mathbb{R}^{C \times K}$ (where C is the number of classes and K is the total concept count). To emulate the Matryoshka behavior, we apply a dynamic masking operation during training. For a given nesting level d , we construct a binary mask $\mathbf{M}_d \in \{0, 1\}^K$ where the first d entries are 1 and the rest are 0. The prediction at level d is computed as:

$$\hat{y}_d = (\mathbf{W}_{\text{shared}} \odot \mathbf{M}_d) \cdot \mathbf{c}_{\text{ord}} \quad (5)$$

where \odot denotes row-wise broadcasting of the mask. During training, our default implementation iterates through all levels in \mathcal{D} and sums their losses for each batch, giving the lowest-dimensional prefixes dense gradient signals. A lighter random-level variant can reduce training cost, but we treat it as an efficiency ablation rather than the default because extreme compression levels are most sensitive to sparse supervision.

Implications and Trade-offs. Weight sharing forces a single matrix to be jointly optimal for early predictions and later refinements, collapsing parameter overhead to $O(C \cdot K)$ and enabling *continuous elasticity* where inference can stop at any integer k . The cost is a small accuracy gap (Section 5), since shared weights cannot specialize per scale, giving practitioners a clean choice between peak accuracy (Standard) and minimum memory footprint (Efficient).

4 Theoretical Analysis

Our empirical results demonstrate that MCBM achieves high accuracy with low intervention costs. In this section, we provide a theoretical foundation for these observations from two perspectives: (1) **Efficiency**, determining the asymptotic scaling of intervention cost, and (2) **Correctness**, establishing an upper bound on classification error under intervention. Detailed proofs are provided in Appendix B and C.

4.1 Asymptotic Intervention Efficiency

MCBM imposes a nested structure on the otherwise flat $O(K)$ intervention budget of standard CBM. We model intervention as a “lazy verification” workflow: inspect ranked concepts from coarse to fine, correct the current prefix, and stop once the prediction is fixed. The stopping level ℓ^* is minimal-sufficient, so the analysis does not require exhausting all concepts. We bound the expected cost $E = \mathbb{E}[N(x, y)]$ under two structural assumptions:

1. **Geometric Concept Growth:** The number of concepts grows as $k_i = k_1 r^{i-1}$ (for rate $r > 1$).

2. **Geometric Information Decay:** The probability of needing to intervene deeper decays as $P(\ell^* = i) \leq C\gamma^{i-1}$ (for decay $\gamma \in (0, 1)$).

The efficiency of MCBM is determined by the interplay between the model’s capacity expansion (r) and its information capture rate ($1/\gamma$). Empirically, this assumption is testable by measuring the distribution of ℓ^* over initially misclassified samples; on CUB, the observed mass concentrates on early levels and follows an exponential trend with fitted $\gamma = 0.9636$ (Appendix D.6).

Theorem 1 (Intervention Efficiency Regimes). *Let $\rho = r\gamma$ be the spectral ratio between concept growth and probability decay. The expected intervention cost E scales with the total concept count K according to three distinct regimes:*

$$E = \begin{cases} \Theta(1) & \text{if } \gamma < 1/r \quad (\text{Efficient Regime}) \\ \Theta(\log K) & \text{if } \gamma = 1/r \quad (\text{Balanced Regime}) \\ \Theta(K^\alpha) & \text{if } \gamma > 1/r \quad (\text{Heavy-Tailed Regime}) \end{cases} \quad (6)$$

where $\alpha = 1 + \log_r \gamma > 0$.

Remark 1. (The Spectral Race) *This theorem frames efficiency as a “race” between adding costs and gaining information.*

- **Balanced** ($\gamma = 1/r$): costs scale as $\Theta(\log K)$, **formally reducing human effort from linear $O(K)$ to logarithmic order.**
- **Efficient** ($\gamma < 1/r$): information capture outpaces growth; costs converge to a constant $\Theta(1)$, surpassing the logarithmic guarantee.
- **Heavy-Tailed** ($\gamma > 1/r$): unordered concepts degrade to polynomial scaling, underscoring the necessity of the mRMR prior.

4.2 Error Reduction Guarantee via Hellman-Raviv

While classical analysis often uses Fano’s Inequality to establish lower bounds on error, we are interested in a sufficiency condition: does intervening on MCBM concepts *guarantee* a reduction in error? We utilize the Hellman-Raviv Inequality to derive an upper bound on the classification error $P_e(k)$ after k interventions.

Theorem 2 (Upper Bound on Intervention Error). *Let ϵ be the intervention shift penalty, defined by the Kullback-Leibler divergence between the training distribution (soft concepts) and the intervention distribution (hard concepts). The probability of error after k interventions is upper-bounded by:*

$$P_e(k) \leq \frac{1}{2} \left(H(Y) - I(Y; \tilde{C}^{(k)}) \right) + \sqrt{\frac{\epsilon}{2}}, \quad (7)$$

where $H(Y)$ is the marginal entropy of the labels and $I(Y; \tilde{C}^{(k)})$ is the mutual information between the labels and the intervened concept vector.

Remark 2. (Justification of Matryoshka Objective) *This theorem provides a rigorous justification for our training objective. To minimize the error bound $P_e(k)$, one must maximize the mutual information $I(Y; \tilde{C}^{(k)})$. Unlike standard CBM that only maximize this for the full vector ($k = K$), the Matryoshka loss explicitly maximizes this mutual information for every prefix $k \in \mathcal{D}$. This guarantees that the error bound tightens monotonically with every additional intervention step.*

Remark 3. (Practical Non-Idealities) *Deep CBMs only approximate the Bayesian classifier used in the Hellman–Raviv argument, and joint training can introduce concept leakage [17]. These gaps are absorbed by ϵ : severe leakage, overfitting, or soft-to-hard intervention shift inflates the KL penalty and loosens the bound. A strictly sequential MCBM that isolates $X \rightarrow C$ from $C \rightarrow Y$ still preserves strong low-budget accuracy in our experiments.*

5 Experiments

We evaluate MCBM on three fine-grained benchmarks, CUB-200-2011 [22], LAD [29], and CelebA [15], around four research questions. **RQ1:** Does a single MCBM match independently

trained models across concept granularities? **RQ2:** Does mRMR ordering reduce the human effort of test-time intervention? **RQ3:** Does MCBM offer a smooth annotation-accuracy trade-off without retraining? **RQ4:** How effectively does mRMR concentrate discriminative information in early dimensions versus random or heuristic orderings?

5.1 Experimental Setup

Datasets and Metrics. We use **CUB** ($K = 112$) [22], **CelebA** ($K = 40$) [15], and **LAD** ($K = 256$) [29]. CelebA is treated as a binary attribute-based benchmark with *Attractive* as the target and the remaining facial attributes as concepts. We report *Accuracy* and *Macro F1*, and *Accuracy@k* (accuracy after correcting the top- k concepts) for intervention efficiency.

Baselines. We compare MCBM against: (1) **Independent CBM**, trained individually for each bottleneck size; (2) **Sequential CBM**, which isolates concept learning from label prediction; (3) **Sparse CBM** and **Label-free CBM** [16]; (4) **Random-Order MCBM**, to ablate the efficacy of mRMR ranking; and (5) **Efficient MCBM**, our weight-tying variant for memory-constrained scenarios. Table 1 reports CUB baselines under the official split.

Implementation. The default backbone is pre-trained Inception_v3 (Sec. 5.4). ResNet-50, Inception_v3, and ViT-B/16 are fine-tuned end-to-end from standard pre-trained weights; CLIP-ViT-B/32 is kept frozen as a zero-shot baseline. Training uses the joint Matryoshka loss (Eq. 2) with dataset-specific nesting dimensions \mathcal{D} .

5.2 Matryoshka Concept Learning Efficacy

We first analyze hierarchical representation learning within a single training run. Table 2 compares *Standard* (independent heads) versus *Efficient MCBM* (weight-tying), while Figure 2 visualizes training dynamics.

Method	Test Acc. (%)
Sparse CBM	53.75
Sequential CBM	69.87
Independent CBM	70.38
Label-free CBM [16]	74.06
MCBM (Standard, $K = 112$)	73.20
Efficient MCBM ($K = 112$)	72.94

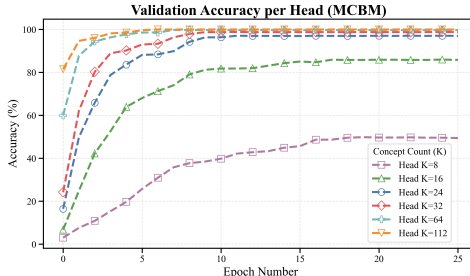


Table 1: **CUB baseline comparison.** Test accuracy under the official split.

Figure 2: **Validation accuracy per head (CUB).** Compressed heads rapidly approach the full model.

Task-Dependent Saturation and Competitive Performance (RQ1). Table 2 reveals distinct saturation patterns: CUB and CelebA plateau early at $K = 32$ and $K = 8$, while LAD requires up to $K = 256$, so a single MCBM can be aggressively truncated for simple tasks and kept full-capacity for complex ones. Figure 2 further shows stable simultaneous convergence across nesting levels, with compressed heads (e.g., $K = 32$) rapidly approaching the full-capacity head ($K = 112$); Efficient MCBM preserves this behavior with only a $\sim 1\%$ drop on LAD, matching independently trained models without maintaining multiple architectures.

5.3 Efficient Concept Intervention

A primary contribution of MCBM is minimizing the cost of human-in-the-loop intervention. We simulate a test-time scenario where a user sequentially corrects mispredicted concepts. Figure 3 compares the efficacy of our *mRMR-based ordering* against a *Random ordering* baseline across CUB, CelebA, and LAD.

Efficiency and Cognitive Load (RQ2). mRMR ordering lowers intervention cost by an order of magnitude versus unordered baselines. On CelebA, MCBM reaches near-perfect accuracy after

merely **3 interventions**, rendering the remaining 37 concepts effectively redundant and validating a “lazy verification” strategy. The advantage persists in complex “threshold regimes” such as LAD ($K = 256$), where mRMR initiates error recovery much earlier (around $k = 125$) than random selection, prioritizing discriminative signals regardless of task complexity.

Head Size (K)	MCBM (Standard)		Efficient MCBM	
	Acc (\uparrow ,%)	F1 (\uparrow ,%)	Acc (\uparrow ,%)	F1 (\uparrow ,%)
CUB Dataset				
$K = 8$	40.94	34.37	38.30	32.23
$K = 16$	63.24	61.39	61.70	59.93
$K = 24$	70.33	69.75	69.31	69.94
$K = 32$	71.80	71.73	71.30	71.33
$K = 64$	73.21	73.19	72.68	72.83
$K = 112$	73.20	73.35	72.94	73.10
LAD Dataset				
$K = 8$	7.76	2.02	7.86	4.07
$K = 16$	14.64	6.62	14.08	8.49
$K = 24$	22.22	14.07	21.22	13.97
$K = 32$	35.40	26.25	35.09	24.57
$K = 64$	67.34	57.64	66.49	53.03
$K = 128$	94.62	93.76	94.15	93.88
$K = 256$	97.89	97.76	97.14	94.91
CelebA Dataset				
$K = 8$	79.40	79.28	79.16	79.13
$K = 16$	79.50	79.41	79.30	79.18
$K = 24$	79.52	79.45	79.26	79.13
$K = 32$	79.52	79.46	79.23	79.09
$K = 40$	79.58	79.51	79.11	78.94

Table 2: **Performance comparison on CUB, LAD, and CelebA.** Accuracy and F1 of Standard and Efficient MCBM across nesting dimensions K . Blue rows highlight the saturation regime where additional heads yield diminishing returns, indicating that a much smaller K already captures most of the achievable accuracy.

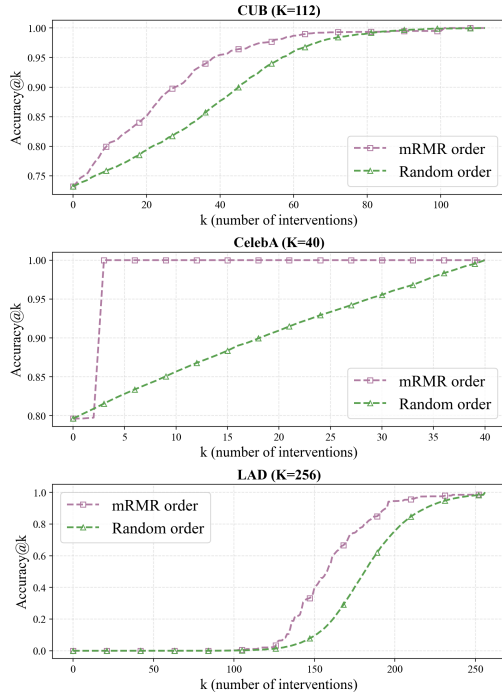


Figure 3: **Intervention efficiency across datasets.** Accuracy@ k vs. intervention count k ; mRMR ordering consistently dominates random ordering.

Dynamic Flexibility and Trade-offs (RQ3). The steep recovery curves make MCBM an “any-time” intervention system: practitioners can adjust intervention depth at test time without retraining, stopping early to secure most of the gains or continuing for higher precision, all within one unified model.

Leakage, Stability, and Matched Heads. Additional CUB diagnostics support that the gains are due to semantic ordering rather than shortcut leakage. The top- K concept predictor remains accurate across budgets (92.44% at $K = 8$, 93.14% at $K = 16$, 93.80% at $K = 32$, and 96.27% at $K = 112$). A strictly Sequential MCBM, which blocks task gradients from reaching the concept extractor, still achieves 72.09% accuracy at $K = 16$ and 73.75% at $K = 112$. The mRMR hierarchy is also stable: across five random seeds, the selected top- K sets for $K \in \{8, 16, 24, 32\}$ have IoU = 1.00, and a full-head weight-based ordering strongly correlates with mRMR (Spearman = 0.934) while yielding a near-identical recovery curve. Finally, using the full $K = 112$ head for partial interventions is inferior to matched Matryoshka heads, dropping from 88.71% to 83.03% at $k = 16$ and from 98.46% to 91.92% at $k = 32$, due to soft/hard concept distribution shift. Full ablations are in Appendix D.

5.4 Impact of Backbone Architecture

To assess the generality of MCBM, we evaluate its performance when scaling the feature extractor across different architectural paradigms. We compare ResNet-18, ResNet-50, Inception_v3, Vision Transformers (ViT-B/16), and a pre-trained Vision-Language model (CLIP-ViT-B/32). Figure 4(a) reports the F1 Score across various nesting levels on the CUB dataset.

Architecture Agnosticism and Inception_v3 Advantage. The “Matryoshka property”—monotonic improvement with concept capacity—holds across CNNs and Transformers, confirming that MCBM

is compatible with modern vision backbones. Among them, Inception_v3 consistently outperforms ResNet-50 and ViT by roughly 5–10% F1, and the gap is most pronounced at low granularities ($K = 8, 16$), suggesting that its multi-scale inception modules align well with the hierarchical nature of fine-grained concept detection.

Limitations of Zero-Shot Features. The frozen CLIP backbone underperforms on this fine-grained task: while vision-language pre-training offers generality, supervised fine-tuning remains essential for capturing subtle attributes such as “beak shape”.

5.5 Impact of Ranking Strategy on Performance

While Section 5.3 demonstrated the benefit of mRMR for *human intervention*, we now investigate its impact on *model representation learning*. We compare two MCBM models trained identically on CUB, differing only in their concept ordering: one uses our proposed mRMR schedule, while the other uses a fixed Random order. Figure 4(b) visualizes the F1 scores across nesting levels.

The Necessity of mRMR for Compression. The results reveal a stark contrast in information density. At low dimensions, the mRMR-based model dominates the random baseline. For instance, at $K = 8$, the Random model collapses to near-chance performance with approximately 3% F1 score, whereas the mRMR model retains a respectable F1 score of nearly 34%. Similarly, at $K = 16$, mRMR outperforms Random by nearly 40 percentage points. This disparity confirms that the “Matryoshka property”, which denotes the ability to perform valid inference at early exits, does not emerge spontaneously from the joint loss alone. It requires the mRMR prior to explicitly guide the compression of semantic information into the earliest dimensions.

As concepts approach the full set ($K = 112$), the gap closes and both methods reach parity ($\sim 75\%$ F1), since ordering becomes irrelevant once the full vocabulary is available—reinforcing that the value of mRMR lies in elasticity, not in peak accuracy.

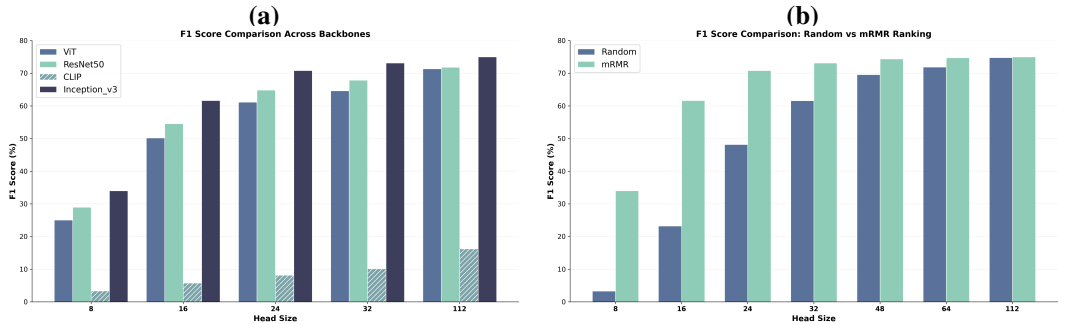


Figure 4: **Backbone and Ranking Effects.** (a) Inception_v3 consistently yields the highest F1, while frozen CLIP struggles with fine-grained attributes. (b) mRMR significantly outperforms random ordering at low dimensions, enabling effective model compression.

Information Concentration (RQ4). mRMR is the structural prior that makes Matryoshka compression usable: the catastrophic collapse of the random baseline at $K = 8$ is a counterfactual proof that joint loss alone does not hierarchically organize the latent space. By front-loading the most discriminative semantic signals, mRMR turns the bottleneck from a flat representation into a strictly ordered hierarchy that both recognizes concepts and encodes their relative importance.

6 Conclusion

We introduce the Matryoshka Concept Bottleneck Models (MCBM), which imposes a nested, information-dense hierarchy on concepts via mRMR. Theoretically, we characterize intervention as a “spectral race”, proving a reduction in human verification costs from linear to logarithmic scales. Empirically, MCBM achieves performance parity with independent baselines while enabling flexible, elastic deployment. Our work effectively bridges the gap between structural efficiency and semantic interpretability, establishing a new standard for scalable human-in-the-loop AI.

References

- [1] M. A. Ahmad, C. Eckert, and A. Teredesai. Interpretable machine learning in healthcare. In *Proceedings of the 2018 ACM International Conference on Bioinformatics, Computational Biology, and Health Informatics*, BCB '18, page 559–560, New York, NY, USA, 2018. Association for Computing Machinery.
- [2] D. Antognini and B. Faltings. Rationalization through concepts. In C. Zong, F. Xia, W. Li, and R. Navigli, editors, *Findings of the Association for Computational Linguistics: ACL-IJCNLP 2021*, pages 761–775, Online, Aug. 2021. Association for Computational Linguistics.
- [3] M. Bhan, Y. Choho, J.-N. Vittaut, N. Chesneau, P. Moreau, and M.-J. Lesot. Towards achieving concept completeness for textual concept bottleneck models. In *Findings of the Association for Computational Linguistics: EMNLP 2025*, pages 2007–2024. Association for Computational Linguistics, 2025.
- [4] K. Chauhan, R. Tiwari, J. Freyberg, P. Shenoy, and K. Dvijotham. Interactive concept bottleneck models. In *Proceedings of the Thirty-Seventh AAAI Conference on Artificial Intelligence and Thirty-Fifth Conference on Innovative Applications of Artificial Intelligence and Thirteenth Symposium on Educational Advances in Artificial Intelligence*, AAAI'23/IAAI'23/EAAI'23. AAAI Press, 2023.
- [5] T. F. Chowdhury, V. M. H. Phan, K. Liao, M.-S. To, Y. Xie, A. van den Hengel, J. W. Verjans, and Z. Liao. AdaCBM: An Adaptive Concept Bottleneck Model for Explainable and Accurate Diagnosis. In *proceedings of Medical Image Computing and Computer Assisted Intervention – MICCAI 2024*, volume LNCS 15010. Springer Nature Switzerland, October 2024.
- [6] R. Daneshjou, K. Vodrahalli, R. A. Novoa, M. Jenkins, W. Liang, V. Rotemberg, J. Ko, S. M. Swetter, E. E. Bailey, O. Gevaert, P. Mukherjee, M. Phung, K. Yekrang, B. Fong, R. Sahasrabudhe, J. A. C. Allerup, U. Okata-Karigane, J. Zou, and A. S. Chiou. Disparities in dermatology ai performance on a diverse, curated clinical image set. *Science Advances*, 8(32), aug 2022.
- [7] G. De Felice, A. Casanova Flores, F. De Santis, S. Santini, J. Schneider, P. Barbiero, and A. Termine. Causally reliable concept bottleneck models. *arXiv preprint arXiv:2503.04363*, 2026.
- [8] C. Ding and H. Peng. Minimum redundancy feature selection from microarray gene expression data. In *Computational Systems Bioinformatics. CSB2003. Proceedings of the 2003 IEEE Bioinformatics Conference. CSB2003*, pages 523–528, 2003.
- [9] M. Havasi, S. Parbhoo, and F. Doshi-Velez. Addressing leakage in concept bottleneck models. In *Proceedings of the 36th International Conference on Neural Information Processing Systems, NIPS '22*, Red Hook, NY, USA, 2022. Curran Associates Inc.
- [10] L. Hu, C. Ren, Z. Hu, H. Lin, C.-L. Wang, Z. Tan, W. Lyu, J. Zhang, H. Xiong, and D. Wang. Editable concept bottleneck models. In *Forty-second International Conference on Machine Learning*, 2025.
- [11] P. W. Koh, T. Nguyen, Y. S. Tang, S. Mussmann, E. Pierson, B. Kim, and P. Liang. Concept bottleneck models. In H. D. III and A. Singh, editors, *Proceedings of the 37th International Conference on Machine Learning*, volume 119 of *Proceedings of Machine Learning Research*, pages 5338–5348. PMLR, 13–18 Jul 2020.
- [12] A. Kusupati, G. Bhatt, A. Rege, M. Wallingford, A. Sinha, V. Ramanujan, W. Howard-Snyder, K. Chen, S. Kakade, P. Jain, and A. Farhadi. Matryoshka representation learning. In S. Koyejo, S. Mohamed, A. Agarwal, D. Belgrave, K. Cho, and A. Oh, editors, *Advances in Neural Information Processing Systems*, volume 35, pages 30233–30249. Curran Associates, Inc., 2022.
- [13] S. Lai, L. Hu, J. Wang, L. Berti-Equille, and D. Wang. Faithful vision-language interpretation via concept bottleneck models. In *The Twelfth International Conference on Learning Representations*, 2024.

- [14] H. Lin, C. Ren, J. Xu, Z. Hu, C.-L. Wang, Y. Shu, H. Xiong, J. Zhang, D. Wang, and L. Hu. Controllable concept bottleneck models. *arXiv preprint arXiv:2601.00451*, 2026.
- [15] Z. Liu, P. Luo, X. Wang, and X. Tang. Deep learning face attributes in the wild. In *Proceedings of International Conference on Computer Vision (ICCV)*, December 2015.
- [16] T. Oikarinen, S. Das, L. M. Nguyen, and T.-W. Weng. Label-free concept bottleneck models. In *The Eleventh International Conference on Learning Representations*, 2023.
- [17] E. Parisini, T. Chakraborti, C. Harbron, B. D. MacArthur, and C. R. S. Banerji. Leakage and interpretability in concept-based models. *arXiv preprint arXiv:2504.14094*, 2025.
- [18] H. Peng, F. Long, and C. Ding. Feature selection based on mutual information criteria of max-dependency, max-relevance, and min-redundancy. *IEEE Transactions on Pattern Analysis and Machine Intelligence*, 27(8):1226–1238, 2005.
- [19] A. Semenov, V. Ivanov, A. Beznosikov, and A. Gasnikov. Sparse concept bottleneck models: Gumbel tricks in contrastive learning, 2024.
- [20] S. Shin, Y. Jo, S. Ahn, and N. Lee. A closer look at the intervention procedure of concept bottleneck models. In A. Krause, E. Brunskill, K. Cho, B. Engelhardt, S. Sabato, and J. Scarlett, editors, *Proceedings of the 40th International Conference on Machine Learning*, volume 202 of *Proceedings of Machine Learning Research*, pages 31504–31520. PMLR, 23–29 Jul 2023.
- [21] M. Vandenhirtz, S. Laguna, R. Marcinkevičs, and J. E. Vogt. Stochastic concept bottleneck models. In *Advances in Neural Information Processing Systems*, 2024.
- [22] C. Wah, S. Branson, P. Welinder, P. Perona, and S. Belongie. The caltech-ucsd birds-200-2011 dataset. Technical Report CNS-TR-2011-001, California Institute of Technology, 2011.
- [23] E. Wong, S. Santurkar, and A. Madry. Leveraging sparse linear layers for debuggable deep networks. In M. Meila and T. Zhang, editors, *Proceedings of the 38th International Conference on Machine Learning*, volume 139 of *Proceedings of Machine Learning Research*, pages 11205–11216. PMLR, 18–24 Jul 2021.
- [24] X. Xu, Y. Qin, L. Mi, H. Wang, and X. Li. Energy-based concept bottleneck models: Unifying prediction, concept intervention, and probabilistic interpretations. In *International Conference on Learning Representations*, 2024.
- [25] Y. Yang, A. Panagopoulou, S. Zhou, D. Jin, C. Callison-Burch, and M. Yatskar. Language in a bottle: Language model guided concept bottlenecks for interpretable image classification. In *Proceedings of the IEEE/CVF Conference on Computer Vision and Pattern Recognition*, pages 19187–19197, 2023.
- [26] J. Yu, Z. Lin, J. Yang, X. Shen, X. Lu, and T. S. Huang. Generative image inpainting with contextual attention. In *Proceedings of the IEEE Conference on Computer Vision and Pattern Recognition (CVPR)*, June 2018.
- [27] M. Yuksekgonul, M. Wang, and J. Zou. Post-hoc concept bottleneck models. In *The Eleventh International Conference on Learning Representations*, 2023.
- [28] M. E. Zarlenga, K. M. Collins, K. D. Dvijotham, A. Weller, Z. Shams, and M. Jamnik. Learning to receive help: intervention-aware concept embedding models. In *Proceedings of the 37th International Conference on Neural Information Processing Systems, NIPS ’23*, Red Hook, NY, USA, 2023. Curran Associates Inc.
- [29] B. Zhao, Y. Fu, R. Liang, J. Wu, Y. Wang, and Y. Wang. A large-scale attribute dataset for zero-shot learning. In *Proceedings of the IEEE Conference on Computer Vision and Pattern Recognition Workshops*, 2019.

A Notation Table

Table 3 summarizes the mathematical notations used throughout the paper.

Table 3: Summary of Notations.

Symbol	Description
<i>Inputs and Model Architecture</i>	
\mathbf{x}, \mathbf{y}	Input image and ground-truth target label
K	Total number of concepts
C	Number of target classes
$g_\theta(\cdot)$	Feature extractor (Backbone) parameterized by θ
\mathbf{l}	Raw, unordered concept logits vector, $\mathbf{l} \in \mathbb{R}^K$
\mathbf{c}_{GT}	Ground-truth concept binary vector
<i>Matryoshka & mRMR Optimization</i>	
Ω	The set of all available concepts
S_t	The set of selected concepts at step t (mRMR)
$I(X; Y)$	Mutual Information between variables X and Y
$\Pi(\cdot)$	Permutation module based on mRMR ranking
\mathbf{c}_{ord}	Ordered concept vector after permutation
\mathcal{D}	Set of predefined nesting granularities (e.g., $\{8, 16, \dots\}$)
d	Index for a specific nesting level / concept budget
$f_{\phi_d}(\cdot)$	Prediction head for nesting level d
\mathbf{M}_d	Binary mask for Efficient MCBM at level d
\mathcal{L}_{total}	Total joint optimization loss
<i>Theoretical Analysis</i>	
ℓ^*	Minimal sufficient intervention level for a specific instance
k_i	Number of concepts at geometric level i
r	Geometric growth rate of concept set size ($r > 1$)
γ	Geometric decay rate of information need ($\gamma \in (0, 1)$)
ρ	Spectral ratio ($\rho = r\gamma$), determining efficiency regimes
E	Expected intervention cost
$P_e(k)$	Classification error probability after k interventions
$\tilde{\mathbf{C}}^{(k)}$	Concept vector intervened up to index k
ϵ	Intervention shift penalty (KL divergence)

B Proof of Intervention Efficiency Regimes

Building upon the intervention reduction established in the previous section, we now provide a rigorous asymptotic analysis of the expected intervention cost E as a function of the total number of concepts K . While the previous section demonstrated that $E < K$, this section categorizes the exact scaling behavior of E . We show that the efficiency of the Matryoshka CBM is determined by a *spectral race* between the growth of the concept sets (model capacity) and the decay of conditional entropy (information capture).

B.1 Setup and Assumptions

We analyze the behavior of the expected intervention cost $E = \sum_{i=1}^L k_i \cdot P(\ell^* = i)$ under the structural constraints imposed by the Matryoshka architecture.

Assumption 1 (Geometric Concept Growth). *The Matryoshka nesting structure is constructed such that the size of the concept set at level i grows geometrically with rate $r > 1$:*

$$k_i = k_1 \cdot r^{i-1}, \quad i = 1, \dots, L. \quad (\text{B.1})$$

Given $k_L = K$, the number of levels scales logarithmically:

$$L = \log_r \left(\frac{K}{k_1} \right) + 1 = \Theta(\log K). \quad (\text{B.2})$$

Assumption 2 (Geometric Probability Decay). *The probability mass function of the minimal sufficient level ℓ^* decays geometrically with rate $\gamma \in (0, 1)$:*

$$P(\ell^* = i) \leq C \cdot \gamma^{i-1}, \quad (\text{B.3})$$

where C is a normalization constant ensuring $\sum P(\ell^* = i) = 1$. The parameter γ represents the information sparsity of the task; a lower γ implies that relevant information is highly concentrated in the first few dimensions.

B.2 Derivation of Convergence Regimes

Theorem 3 (General Intervention Cost Bound). *Under Assumptions 1 and 2, the expected intervention cost E is bounded by a geometric series governed by the spectral ratio $\rho = r\gamma$:*

$$E \leq Ck_1 \sum_{i=1}^L (r\gamma)^{i-1}. \quad (\text{B.4})$$

Proof. Substituting the definitions of k_i and $P(\ell^* = i)$ into the expectation:

$$\begin{aligned} E &= \sum_{i=1}^L k_i \cdot P(\ell^* = i) \leq \sum_{i=1}^L (k_1 r^{i-1}) (C\gamma^{i-1}) \\ &= Ck_1 \sum_{i=1}^L (r\gamma)^{i-1}. \end{aligned} \quad (\text{B.5})$$

Let $\rho = r\gamma$. The summation $S_L = \sum_{j=0}^{L-1} \rho^j$ behaves differently depending on whether ρ is below, equal to, or above 1. \square

Remark 4. *The term $\rho = r\gamma$ represents the ratio between the **cost expansion rate** (r) and the **information gain rate** ($1/\gamma$). If $\rho < 1$, information is gained faster than cost is added; if $\rho > 1$, cost outpaces information.*

Corollary 4 (Intervention Efficiency Regimes). *The asymptotic scaling of E in K falls into one of three regimes:*

1. **Efficient regime** ($\gamma < 1/r$): $E = \Theta(1)$.
2. **Balanced regime** ($\gamma = 1/r$): $E = \Theta(\log K)$.
3. **Heavy-tailed regime** ($\gamma > 1/r$): $E = \Theta(K^\alpha)$, where $\alpha = 1 + \log_r \gamma > 0$.

Proof. We analyze $S_L = \sum_{i=1}^L \rho^{i-1}$ from (B.4) for each case.

Case 1: $\rho < 1$. The geometric series converges:

$$S_L = \frac{1 - \rho^L}{1 - \rho} < \frac{1}{1 - \rho}, \quad E \leq \frac{Ck_1}{1 - r\gamma} = \Theta(1). \quad (\text{B.6})$$

Case 2: $\rho = 1$. Every term equals 1, so $S_L = L$, and using Assumption 1:

$$E \approx Ck_1 L = Ck_1 \left(\log_r \frac{K}{k_1} + 1 \right) = \Theta(\log K). \quad (\text{B.7})$$

Case 3: $\rho > 1$. The series diverges geometrically:

$$S_L = \frac{\rho^L - 1}{\rho - 1} \approx \frac{\rho^L}{\rho - 1} = \Theta(\rho^L). \quad (\text{B.8})$$

Since $r^L \propto K$ and $\gamma^L = (K/k_1)^{\log_r \gamma} \propto K^{\log_r \gamma}$, we get

$$E \propto K \cdot K^{\log_r \gamma} = K^{1 + \log_r \gamma}. \quad (\text{B.9})$$

With $\gamma > 1/r$ we have $\log_r \gamma > -1$, so $\alpha = 1 + \log_r \gamma > 0$. \square

Remark 5. *These regimes give a concrete target for Matryoshka Representation Learning:*

- **Regime 1** ($\Theta(1)$): *the ideal state—a critical mass of discriminative information has been compressed into the first k_1 dimensions, and the system is fully scalable in K .*
- **Regime 2** ($\Theta(\log K)$): *value of an extra concept just offsets its verification cost.*
- **Regime 3** ($\Theta(K^\alpha)$): *information bottleneck failure; the nested structure offers little gain over a flat baseline.*

C Proof of Intervention Reduction

We provide a formal proof that intervening on concepts in a Matryoshka CBM strictly reduces the upper bound on classification error, using the Hellman–Raviv inequality.

C.1 Preliminaries and Definitions

Let data be sampled from P over $\mathcal{X} \times \mathcal{Y} \times \{0, 1\}^K$, where $X \in \mathcal{X}$, $Y \in [C]$, and $C^* \in \{0, 1\}^K$ is the ground-truth concept vector. The MCBM consists of:

1. A concept encoder $g : \mathcal{X} \rightarrow \mathbb{R}^K$ with $\hat{C} = \sigma(g(X))$.
2. A label predictor $f : \mathbb{R}^K \rightarrow \Delta^{C-1}$.

Definition 1 (Intervention Vector). Let $\tilde{C}^{(k)}$ denote the concept vector after intervening on the first k concepts under the Matryoshka ordering \mathcal{M} :

$$\tilde{C}^{(k)} = [c_1^*, \dots, c_k^*, \hat{c}_{k+1}, \dots, \hat{c}_K]. \quad (\text{C.1})$$

Definition 2 (Intervention Error).

$$P_e(k) = \mathbb{P}(f(\tilde{C}^{(k)}) \neq Y) = \mathbb{E}[\mathbb{I}(f(\tilde{C}^{(k)}) \neq Y)]. \quad (\text{C.2})$$

C.2 Error Bound Derivation

Lemma 5 (Hellman–Raviv Inequality). For any Bayesian classifier predicting Y from observation Z , the error probability satisfies (in nats)

$$P_e \leq \frac{1}{2}H(Y | Z). \quad (\text{C.3})$$

Remark 6. Reducing the conditional entropy $H(Y | Z)$ strictly lowers the ceiling on the error.

Theorem 6 (Upper Bound on Intervention Error). Let $\epsilon = D_{KL}(P_{int} \| P_{train})$ be the intervention shift penalty. The probability of error after k interventions satisfies

$$P_e(k) \leq \frac{1}{2}(H(Y) - I(Y; \tilde{C}^{(k)})) + \sqrt{\frac{\epsilon}{2}}. \quad (\text{C.4})$$

Proof. **Step 1.** By Lemma 5,

$$P_e(k) \leq \frac{1}{2}H(Y | \tilde{C}^{(k)}). \quad (\text{C.5})$$

Step 2. Using $I(Y; Z) = H(Y) - H(Y | Z)$,

$$H(Y | \tilde{C}^{(k)}) = H(Y) - I(Y; \tilde{C}^{(k)}), \quad (\text{C.6})$$

yielding the entropic part of the bound. **Step 3.** The classifier f is trained under P_{train} but evaluated under P_{int} . By Pinsker’s inequality, the total-variation gap is bounded by

$$\delta(P_{int}, P_{train}) \leq \sqrt{\frac{1}{2}D_{KL}(P_{int} \| P_{train})} = \sqrt{\frac{\epsilon}{2}}, \quad (\text{C.7})$$

which, when added to the previous bound, gives (C.4). \square

Remark 7. Equation (C.4) mathematically justifies the Matryoshka objective: minimizing $P_e(k)$ requires maximizing $I(Y; \tilde{C}^{(k)})$ for every prefix $k \in \mathcal{M}$, which standard CBM does only for $k = K$.

Corollary 7 (Monotonic Error Reduction). Since $I(Y; \tilde{C}^{(k+1)}) \geq I(Y; \tilde{C}^{(k)})$, the upper bound on the classification error is non-increasing in the intervention depth k .

Remark 8. This guarantees that any-time intervention is safe: stopping at depth k never makes the theoretical bound worse than at depth $k - 1$.

D Supplementary Rebuttal Experiments

D.1 CUB Baselines and Official Split Protocol

Table 4 expands the CUB baseline comparison in the main paper. Sparse CBM is reproduced on the official CUB split because the original random split can leak test images into model selection. Label-free CBM obtains strong task accuracy, but its CLIP-aligned concepts are not guaranteed to match the human-annotated CUB concept vocabulary; therefore, they are less reliable for expert intervention than the fully grounded concepts used by MCBM.

Table 4: **Comparison with CBM baselines on CUB under the official split.**

Method	Test Acc. (%)	Remark
Sparse CBM	53.75	Reproduced on the official CUB split
Sequential CBM	69.87	Standard CBM baseline
Independent CBM	70.38	Standard CBM baseline
Label-free CBM [16]	74.06	Semantically ambiguous for intervention
MCBM (Standard, $K = 112$)	73.20	Ours
Efficient MCBM ($K = 112$)	72.94	Ours

D.2 Concept Accuracy and Leakage Analysis

Jointly trained CBMs can leak task information through concepts that no longer behave as human-interpretable attributes [17]. We check this in two ways. First, the $X \rightarrow C$ predictor remains accurate on the top mRMR prefixes: 92.44% at $K = 8$, 93.14% at $K = 16$, 93.80% at $K = 32$, and 96.27% at $K = 112$. Second, we train a strictly Sequential MCBM in which the concept extractor is trained before the Matryoshka task heads, removing gradient paths from the task loss into the concept representation. Even under this zero-leakage protocol, the model reaches 72.09% task accuracy at $K = 16$ and 73.75% at $K = 112$, showing that low-budget recovery is driven primarily by semantic compression through the mRMR order.

We also compare a flat joint CBM trained only with $K = 16$ concepts against the matched $d = 16$ Matryoshka head. The flat joint model reaches 65.84% accuracy, whereas the matched Matryoshka head reaches 63.24%. This gap is expected: the flat model has more freedom to distort its small concept set for task prediction, while nested supervision from larger heads regularizes MCBM toward a shared semantic ordering.

D.3 Efficient MCBM Training Strategy

The default Efficient MCBM iterates over all nesting levels in each batch. To quantify the cost of this dense supervision, we compare it with a random-level variant that samples one granularity per batch. Random-level training is about $2.35\times$ faster, but Table 5 shows that it damages the lowest budgets, where dense gradients are most important for enforcing the Matryoshka prior.

Table 5: **Sensitivity of Efficient MCBM to training strategy on CUB.** Negative deltas indicate degradation from all-level training to random-level sampling.

K	Accuracy (%)			Macro F1 (%)		
	All Levels	Random Level	Δ	All Levels	Random Level	Δ
8	55.49	25.70	-29.79	45.05	15.95	-29.10
16	88.57	70.69	-17.88	84.85	62.95	-21.90
32	98.46	96.93	-1.54	98.09	96.08	-2.01
64	99.50	99.50	0.00	99.34	99.34	0.00
112	100.00	99.50	-0.50	100.00	99.34	-0.66

D.4 mRMR Stability and Weight-Based Ordering

To test whether the static hierarchy is brittle under redundant concepts, we rerun mRMR on CUB with five random seeds and compute the Intersection over Union of the top prefixes. The selected top- K sets for $K = 8, 16, 24, 32$ have IoU = 1.00 across all runs, indicating that the high-value prefix is stable even if long-tail concepts can permute.

We further compare mRMR against a task-weight ordering extracted from a fully trained independent $K = 112$ CBM head. Ranking concepts by $\sum_c |W_{c,i}|$ yields Spearman correlation 0.934 and Kendall’s $\tau = 0.792$ with mRMR ($p < 10^{-30}$), and gives a near-identical intervention recovery curve. Thus, mRMR anticipates the same task-relevance hierarchy that a full predictor learns, without requiring a separate full-capacity CBM to be trained first.

D.5 Matched-Head Versus Cross-Head Intervention

One alternative is to intervene on the first k concepts but still run the full $K = 112$ classifier. This mixes k hard expert labels with $K - k$ soft predicted logits, producing a distribution shift. Table 6 compares matched Matryoshka heads against the full head under this cross-head protocol.

Table 6: **Cross-head intervention on CUB.** Matched heads are trained for the exact corrected prefix size, while the full head receives a mixture of corrected and uncorrected concepts.

Corrected k	Matched Head Acc.	Full Head Acc.	Drop
16	88.71	83.03	-5.68
32	98.46	91.92	-6.54

D.6 Empirical Geometric Decay

For each initially misclassified CUB sample, we record the minimal sufficient intervention level ℓ^* at which the prediction becomes correct. Figure 5 plots the cumulative recovery curve, marginal gain, and fitted distribution of ℓ^* . The fitted exponential trend has $\gamma = 0.9636$ with $R^2 = 0.4808$. The moderate R^2 reflects local long-tail spikes from coupled fine-grained attributes, but the macro trend still concentrates mass on early interventions, supporting the geometric-decay assumption used in Theorem 1.

D.7 Causal CBM Comparison

Causal and stochastic CBMs are complementary to MCBM. A causal graph can propagate a corrected concept to dependent concepts, improving inter-concept consistency. However, reading a graph backward from the task node identifies a Markov blanket, not an ordered subset optimized for a fixed budget. If multiple parents are redundant, verifying all of them wastes scarce expert attention. mRMR directly optimizes the prefix for maximum relevance and minimum redundancy.

The deployment distinction is also important. Dynamic graph-based methods generally keep the full concept vocabulary, graph structure, and propagation machinery active at inference time. They can mask or prioritize concepts logically, but the full model remains in memory. MCBM turns the ranking into an architectural prefix: when the budget is k , suffix concepts and unmatched heads can be removed, giving predictable physical truncation for edge or clinical deployments.

E Limitations

MCBM inherits several limitations from concept bottleneck modeling. First, its interpretability and intervention value depend on the quality and completeness of the concept vocabulary: missing, biased, or ambiguous concepts can limit both accuracy and human trust. Second, the theoretical efficiency guarantees rely on geometric information concentration in the ordered prefixes; our CUB analysis supports this trend empirically, but tasks with highly diffuse or weakly predictive concepts may fall into the heavier-tailed regimes described in Section 4. Third, although we evaluate multiple datasets and backbones, the experiments focus on visual attribute benchmarks, so further validation is needed before deployment in clinical, scientific, or other high-stakes domains. Finally, physical truncation reduces memory and intervention cost, but it does not remove the need for domain-specific auditing, calibration, fairness evaluation, and expert oversight when the model is used in real decision pipelines.

F Broader Impact

MCBM can lower the cost of expert oversight by allowing practitioners to inspect a small, ordered prefix of human-understandable concepts before deciding whether further intervention is needed. This may improve accessibility of interpretable models in resource-constrained or high-stakes settings. At the same time, cheaper intervention does not remove the need for dataset and concept-set auditing: biased concept annotations, incomplete concept vocabularies, or over-reliance on imperfect concept

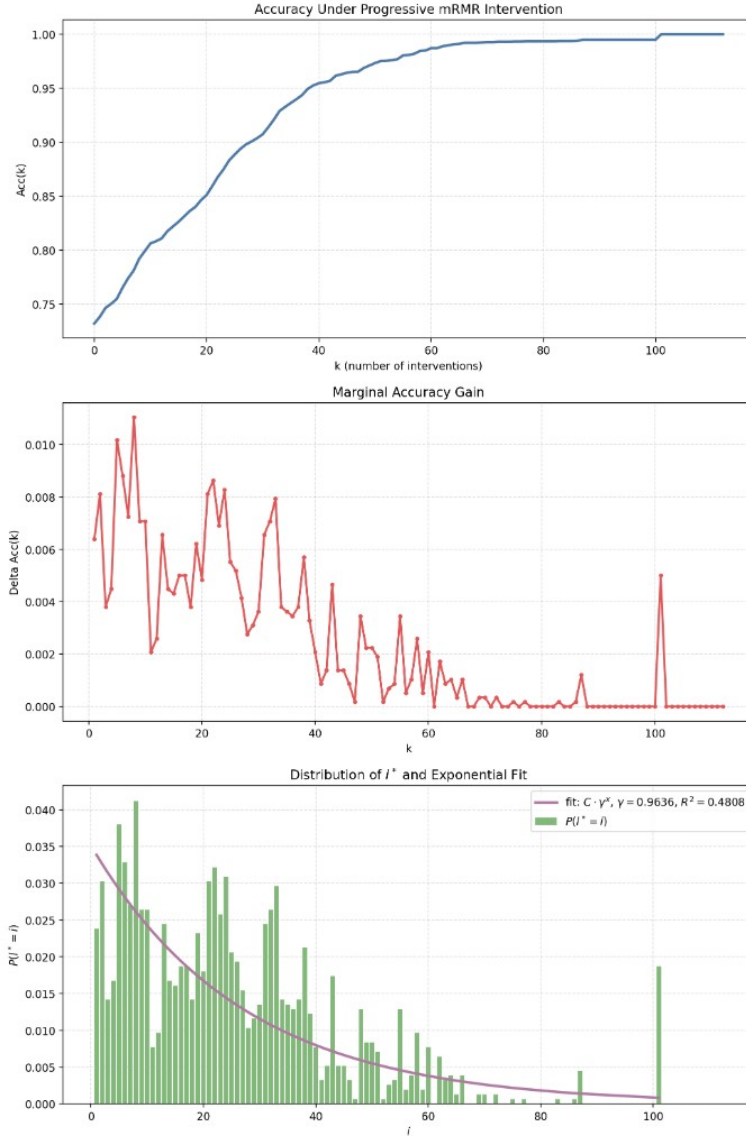


Figure 5: **Empirical geometric decay on CUB.** Accuracy recovers rapidly under progressive mRMR intervention; marginal gains decay overall, and the stopping-level distribution follows an exponential trend.

predictions could still lead to unfair or unsafe decisions. We therefore view MCBM as a tool for reducing verification burden, not as a replacement for domain expert review, fairness evaluation, or deployment-specific risk assessment.

G Licenses and Existing Assets

This paper and our original accompanying materials are released under the CC-BY 4.0 license. We use only public research assets cited in the main paper, including CUB-200-2011, LAD, CelebA, ImageNet-pretrained backbones, and prior CBM baselines, and we respect their original licenses and terms of use. Third-party datasets, pretrained weights, and baseline implementations remain governed by their original creators' licenses and are not redistributed as new assets.

H mRMR Concept Ranking for CUB Dataset

This section presents the complete ranked list of 112 concepts for the CUB-200-2011 dataset, ordered by their mRMR score. The ranking is computed using the Minimum Redundancy Maximum Relevance algorithm as described in Section 3. Table 7 details the Rank, Concept Name, mRMR Score ($I(c_i; y) - \text{Redundancy}$), Relevance ($I(c_i; y)$), and Redundancy ($\frac{1}{|S|} \sum I(c_i; c_j)$) for each attribute.

Table 7: **Full mRMR Concept Ranking for CUB Dataset.** Attributes are ordered by decreasing information density.

Rank	Concept	Score	Relevance	Redundancy
1	has_shape::perching-like	0.6931	0.6931	0.0000
2	has_bill_color::orange	0.6884	0.6930	0.0046
3	has_underparts_color::black	0.6769	0.6830	0.0061
4	has_upperparts_color::orange	0.6726	0.6760	0.0035
5	has_belly_color::buff	0.6739	0.6823	0.0084
6	has_bill_shape::spatulate	0.6615	0.6762	0.0146
7	has_back_pattern::multi-colored	0.6580	0.6830	0.0249
8	has_size::large_(16_-_32_in)	0.6433	0.6577	0.0144
9	has_under_tail_color::orange	0.6330	0.6679	0.0349
10	has_underparts_color::buff	0.6310	0.6493	0.0182
11	has_shape::swallow-like	0.6350	0.6733	0.0383
12	has_belly_color::black	0.6307	0.6764	0.0457
13	has_wing_color::orange	0.6274	0.6764	0.0490
14	has_bill_length::longer_than_head	0.6189	0.6596	0.0407
15	has_throat_color::black	0.6107	0.6580	0.0472
16	has_forehead_color::orange	0.6078	0.6394	0.0316
17	has_crown_color::orange	0.5853	0.6360	0.0508
18	has_breast_color::black	0.5881	0.6584	0.0703
19	has_eye_color::buff	0.5884	0.6420	0.0536
20	has_upperparts_color::rufous	0.5796	0.5834	0.0037
21	has_tail_shape::rounded_tail	0.5785	0.6028	0.0242
22	has_leg_color::orange	0.5786	0.5909	0.0123
23	has_upper_tail_color::orange	0.5660	0.6129	0.0469
24	has_crown_color::buff	0.5534	0.5805	0.0271
25	has_back_color::rufous	0.5510	0.5696	0.0185
26	has_tail_pattern::multi-colored	0.5481	0.5654	0.0173
27	has_wing_color::blue	0.5355	0.5578	0.0223
28	has_primary_color::orange	0.5335	0.5906	0.0572
29	has_bill_shape::all-purpose	0.5227	0.5556	0.0329
30	has_back_color::orange	0.5232	0.5807	0.0576
31	has_leg_color::rufous	0.5215	0.5275	0.0060
32	has_wing_pattern::striped	0.5202	0.5292	0.0091
33	has_wing_color::rufous	0.5184	0.5399	0.0215
34	has_head_pattern::eyering	0.5093	0.5230	0.0137
35	has_upperparts_color::blue	0.5071	0.5411	0.0340
36	has_primary_color::rufous	0.4985	0.5228	0.0243
37	has_back_color::blue	0.4958	0.5352	0.0394
38	has_wing_color::black	0.4924	0.5056	0.0132
39	has_nape_color::orange	0.4866	0.5351	0.0485
40	has_wing_pattern::spotted	0.4774	0.5009	0.0235
41	has_primary_color::black	0.4740	0.5052	0.0313
42	has_throat_color::orange	0.4635	0.4983	0.0349
43	has_upper_tail_color::rufous	0.4568	0.4740	0.0172
44	has_primary_color::blue	0.4489	0.4866	0.0377
45	has_nape_color::black	0.4487	0.4785	0.0298

C continued on next page

Table 7 – continued from previous page

Rank	Concept	Score	Relevance	Redundancy
46	has_size::very_large_(32_-_72_in)	0.4433	0.4764	0.0331
47	has_upperparts_color::black	0.4395	0.4641	0.0246
48	has_nape_color::rufous	0.4341	0.4491	0.0150
49	has_wing_shape::rounded-wings	0.4193	0.4236	0.0043
50	has_upper_tail_color::blue	0.4192	0.4572	0.0380
51	has_breast_color::orange	0.4139	0.4441	0.0302
52	has_under_tail_color::black	0.4109	0.4373	0.0263
53	has_under_tail_color::rufous	0.4075	0.4244	0.0169
54	has_belly_color::grey	0.4024	0.4173	0.0150
55	has_underparts_color::red	0.4004	0.4156	0.0151
56	has_underparts_color::orange	0.3960	0.4303	0.0342
57	has_breast_color::grey	0.3956	0.4166	0.0210
58	has_under_tail_color::blue	0.3924	0.4250	0.0326
59	has_underparts_color::grey	0.3827	0.4083	0.0256
60	has_crown_color::blue	0.3810	0.4150	0.0339
61	has_tail_pattern::striped	0.3792	0.3887	0.0095
62	has_bill_color::rufous	0.3714	0.3800	0.0086
63	has_forehead_color::blue	0.3675	0.4058	0.0383
64	has_wing_color::red	0.3607	0.3878	0.0270
65	has_nape_color::blue	0.3567	0.3853	0.0286
66	has_upperparts_color::red	0.3535	0.3783	0.0248
67	has_primary_color::grey	0.3527	0.3798	0.0271
68	has_breast_color::red	0.3509	0.3700	0.0191
69	has_forehead_color::rufous	0.3469	0.3586	0.0117
70	has_back_pattern::spotted	0.3460	0.3685	0.0225
71	has_upper_tail_color::black	0.3443	0.3658	0.0216
72	has_belly_color::orange	0.3441	0.3752	0.0311
73	has_crown_color::rufous	0.3440	0.3586	0.0147
74	has_back_color::black	0.3412	0.3658	0.0246
75	has_belly_color::red	0.3381	0.3585	0.0203
76	has_leg_color::red	0.3308	0.3459	0.0150
77	has_back_color::red	0.3219	0.3476	0.0258
78	has_throat_color::grey	0.3194	0.3382	0.0188
79	has_underparts_color::rufous	0.3122	0.3199	0.0076
80	has_size::medium_(9_-_16_in)	0.3106	0.3168	0.0062
81	has_primary_color::red	0.2896	0.3053	0.0157
82	has_breast_color::rufous	0.2882	0.2964	0.0082
83	has_bill_shape::curved_(up_or_down)	0.2797	0.2920	0.0123
84	has_breast_pattern::striped	0.2771	0.2817	0.0045
85	has_belly_color::rufous	0.2757	0.2866	0.0109
86	has_nape_color::red	0.2759	0.2914	0.0155
87	has_under_tail_color::red	0.2701	0.2904	0.0203
88	has_upperparts_color::grey	0.2695	0.2817	0.0122
89	has_forehead_color::black	0.2682	0.2888	0.0206
90	has_upper_tail_color::red	0.2677	0.2904	0.0227
91	has_forehead_color::grey	0.2569	0.2683	0.0113
92	has_breast_pattern::spotted	0.2487	0.2632	0.0144
93	has_back_pattern::striped	0.2466	0.2536	0.0070
94	has_crown_color::black	0.2460	0.2638	0.0178
95	has_tail_pattern::spotted	0.2328	0.2429	0.0101
96	has_breast_color::blue	0.2261	0.2423	0.0162
97	has_throat_color::red	0.2214	0.2400	0.0186
98	has_wing_color::grey	0.2179	0.2292	0.0113
99	has_nape_color::grey	0.2142	0.2285	0.0144
100	has_underparts_color::blue	0.2135	0.2285	0.0150

C continued on next page

Table 7 – continued from previous page

Rank	Concept	Score	Relevance	Redundancy
101	has_bill_shape::needle	0.2133	0.2248	0.0115
102	has_bill_color::red	0.2032	0.2124	0.0092
103	has_crown_color::grey	0.2018	0.2141	0.0123
104	has_belly_color::blue	0.1975	0.2117	0.0142
105	has_bill_length::shorter_than_head	0.1938	0.1994	0.0056
106	has_shape::long-legged-like	0.1920	0.1977	0.0057
107	has_bill_color::buff	0.1920	0.1994	0.0074
108	has_head_pattern::unique_pattern	0.1917	0.1984	0.0067
109	has_throat_color::rufous	0.1910	0.1977	0.0066
110	has_wing_pattern::solid	0.1896	0.1967	0.0071
111	has_back_color::grey	0.1862	0.2009	0.0147
112	has_eye_color::orange	0.1523	0.1588	0.0065

I mRMR Concept Ranking for CelebA Dataset

This section presents the complete ranked list of 40 binary attributes for the CelebA dataset. As shown in the experiments, the top-ranked concepts (e.g., “Attractive”, “Young”, “Heavy_Makeup”) carry the vast majority of the discriminative information for identity-related tasks, explaining the rapid performance saturation observed at $K = 8$.

Table 8: **Full mRMR Concept Ranking for CelebA Dataset.** Attributes are ordered by decreasing information density.

Rank	Concept	Score	Relevance	Redundancy
1	Attractive	0.6928	0.6928	0.0000
2	5_o_Clock_Shadow	0.0000	0.0020	0.0020
3	Young	0.0403	0.0808	0.0404
4	Heavy_Makeup	0.0501	0.1205	0.0704
5	Chubby	0.0128	0.0344	0.0217
6	Blurry	0.0117	0.0182	0.0065
7	Eyeglasses	0.0142	0.0283	0.0141
8	Wearing_Lipstick	0.0246	0.1204	0.0958
9	Pointy_Nose	0.0121	0.0266	0.0145
10	Big_Nose	0.0126	0.0395	0.0269
11	Oval_Face	0.0114	0.0191	0.0077
12	Gray_Hair	0.0115	0.0252	0.0137
13	Receding_Hairline	0.0086	0.0168	0.0082
14	Double_Chin	0.0086	0.0266	0.0179
15	Arched_Eyebrows	0.0095	0.0323	0.0228
16	Wavy_Hair	0.0089	0.0235	0.0146
17	Wearing_Hat	0.0059	0.0102	0.0043
18	Bald	0.0062	0.0132	0.0070
19	Male	0.0090	0.0800	0.0710
20	Smiling	0.0057	0.0110	0.0053
21	Brown_Hair	0.0041	0.0088	0.0048
22	Rosy_Cheeks	0.0032	0.0146	0.0113
23	Mustache	0.0029	0.0106	0.0077
24	Pale_Skin	0.0028	0.0038	0.0010
25	Narrow_Eyes	0.0018	0.0027	0.0009
26	Bags_Under_Eyes	0.0020	0.0161	0.0141
27	Blond_Hair	0.0020	0.0123	0.0103
28	Goatee	0.0009	0.0113	0.0103

Continued on next page

Table 8 – continued from previous page

Rank	Concept	Score	Relevance	Redundancy
29	Wearing_Necktie	0.0005	0.0128	0.0123
30	Bangs	-0.0019	0.0018	0.0037
31	Big_Lips	-0.0020	0.0020	0.0040
32	Straight_Hair	-0.0025	0.0009	0.0033
33	Bushy_Eyebrows	-0.0035	0.0009	0.0044
34	Sideburns	-0.0040	0.0051	0.0091
35	Wearing_Necklace	-0.0041	0.0024	0.0065
36	High_Cheekbones	-0.0041	0.0112	0.0153
37	Wearing_Earrings	-0.0049	0.0078	0.0127
38	Black_Hair	-0.0051	0.0000	0.0051
39	No_Beard	-0.0076	0.0200	0.0276
40	Mouth_Slightly_Open	-0.0080	0.0002	0.0082

J mRMR Concept Ranking for LAD Dataset

This section presents the complete ranked list of 359 concepts for the Large-scale Attribute Dataset (LAD), ordered by their mRMR score. The hierarchy reflects the “Threshold Effect” observed in our experiments, where early concepts capture broad, structural attributes (e.g., “material”, “state”), while later concepts refine specific details.

Table 9: **Full mRMR Concept Ranking for LAD Dataset.** Attributes are ordered by decreasing information density.

Rank	Concept	Score	Relevance	Redundancy
1	current state: is complete	0.5517	0.5517	0.0000
2	material: is made of metal	0.4689	0.5473	0.0784
3	material: is made of metal	0.4538	0.5228	0.0691
4	other body parts: has eyes	0.3893	0.4355	0.0462
5	taste: tastes sweet	0.3802	0.5449	0.1647
6	aim: is for family	0.3860	0.5410	0.1550
7	price: is expensive	0.3871	0.5195	0.1323
8	edibility: is common	0.3719	0.5383	0.1664
9	aim: is for display	0.3674	0.5225	0.1551
10	function: can be driven	0.3632	0.5174	0.1542
11	growth: grows on trees	0.3683	0.5070	0.1386
12	safety: is safe	0.3662	0.5218	0.1556
13	edibility: has a high water content	0.3631	0.5294	0.1663
14	material: is made of plastic	0.3617	0.5003	0.1386
15	aim: is for business	0.3601	0.5422	0.1821
16	epidermis: has peel	0.3558	0.4970	0.1411
17	function: can move	0.3577	0.5181	0.1604
18	aim: is for personal	0.3552	0.5410	0.1858
19	current state: is raw	0.3581	0.5458	0.1876
20	other body parts: has a nose	0.3530	0.4088	0.0558
21	parts: has seats	0.3570	0.5075	0.1505
22	material: is made of plastic	0.3579	0.5473	0.1894
23	habit: is active	0.3443	0.4073	0.0630
24	existence: is common	0.3485	0.5468	0.1983
25	parts: has a engine	0.3518	0.4923	0.1405
26	hardness: is soft	0.3523	0.4600	0.1077
27	epidermis: is smooth	0.3473	0.4566	0.1093
28	shape: is long	0.3486	0.4837	0.1350

Continued on next page

Table 9 – continued from previous page

Rank	Concept	Score	Relevance	Redundancy
29	existence: is movable	0.3501	0.4803	0.1302
30	size: is small (compared to apples)	0.3474	0.4486	0.1011
31	parts: has lights	0.3483	0.4899	0.1416
32	edibility: can be eaten directly	0.3453	0.4470	0.1017
33	aim: is for office use	0.3479	0.4698	0.1219
34	function: can carry a small number (226410) of passengers	0.3422	0.4479	0.1057
35	size: is big (compared to a mobile phone)	0.3424	0.4437	0.1013
36	fitness: fits people with a pointed nose	0.3422	0.3721	0.0299
37	other body parts: has a backbone	0.3415	0.4009	0.0594
38	aim: is for civil use	0.3424	0.4374	0.0950
39	power: is a low-power (2264100 w) device	0.3412	0.4424	0.1012
40	weight: weighs tons	0.3421	0.4565	0.1144
41	appearance: has soft skin	0.3382	0.3911	0.0529
42	speed: moves fast	0.3404	0.4613	0.1209
43	sound: is quiet	0.3394	0.4238	0.0844
44	edibility: has seeds	0.3401	0.4066	0.0665
45	shape: is globular	0.3393	0.4161	0.0769
46	parts: has indicator lights	0.3377	0.4217	0.0839
47	other body parts: has a tongue	0.3326	0.3931	0.0605
48	parts: has doors	0.3343	0.4382	0.1040
49	taste: tastes sour	0.3307	0.4060	0.0753
50	parts: has a horn	0.3321	0.4297	0.0976
51	parts: has keys	0.3325	0.4137	0.0812
52	fitness: fits fair-skinned people	0.3311	0.3638	0.0327
53	habit: moves fast	0.3315	0.3868	0.0553
54	color: is black	0.3320	0.4191	0.0871
55	parts: has windows	0.3332	0.4355	0.1023
56	edibility: needs to be skinned	0.3295	0.3813	0.0519
57	habit: has muscle	0.3286	0.3927	0.0641
58	size: is big (compared to cars)	0.3292	0.4146	0.0854
59	edibility: has nutlets	0.3251	0.3809	0.0557
60	parts: has a brake	0.3248	0.4081	0.0832
61	feeling: is lively	0.3216	0.3549	0.0333
62	other body parts: has ears	0.3206	0.3849	0.0643
63	parts: has a plug	0.3207	0.3791	0.0584
64	habit: is friendly	0.3189	0.3685	0.0497
65	usage scenarios: can be used on urban roads	0.3190	0.3963	0.0772
66	function: can give out lights	0.3189	0.3835	0.0646
67	safety: is safe	0.3166	0.3929	0.0763
68	habitat: lives on the ground	0.3149	0.3655	0.0507
69	fitness: fits people with small eyes	0.3150	0.3502	0.0352
70	habit: lives in groups	0.3128	0.3566	0.0438
71	habit: is quiet	0.3104	0.3533	0.0429
72	outside color: is yellow	0.3105	0.3510	0.0406
73	size: is small (compared to pigs)	0.3095	0.3543	0.0448
74	habit: is warm-blooded	0.3049	0.3696	0.0647
75	growth: is tropical	0.3038	0.3423	0.0385
76	habit: is weak	0.3003	0.3472	0.0469
77	diet: eats meat	0.2991	0.3514	0.0524
78	weight: weighs kilograms	0.2994	0.3501	0.0507
79	parts: has a steering wheel	0.2999	0.3659	0.0660
80	function: can carry a large quantity (> 1 tons) of goods	0.2955	0.3505	0.0550
81	medicinal property: is cool or cold	0.2949	0.3303	0.0354
82	hardness: is hard	0.2944	0.3240	0.0297

Continued on next page

Table 9 – continued from previous page

Rank	Concept	Score	Relevance	Redundancy
83	usage scenarios: can be used on rural roads	0.2932	0.3548	0.0616
84	fitness: fits people with ear rings	0.2922	0.3212	0.0290
85	neck: has a long neck	0.2900	0.3466	0.0566
86	power: consumes diesel oil	0.2884	0.3482	0.0598
87	behaviour: can walk	0.2869	0.3400	0.0531
88	smell: is fragrant	0.2860	0.3200	0.0340
89	fitness: fits people with heavy make-up	0.2861	0.3170	0.0308
90	diet: eats plants	0.2865	0.3348	0.0484
91	color: is gray	0.2832	0.3217	0.0385
92	habit: is timid	0.2822	0.3230	0.0407
93	paws: has paws	0.2815	0.3395	0.0581
94	outside color: is red	0.2809	0.3128	0.0319
95	medicinal property: is warm or hot	0.2766	0.3069	0.0303
96	shape: is long	0.2752	0.3020	0.0268
97	teeth: has teeth	0.2751	0.3235	0.0484
98	diet: eats leaves	0.2723	0.3210	0.0487
99	parts: has a number plate	0.2725	0.3257	0.0532
100	feeling: is sexy	0.2690	0.2951	0.0261
101	epidermis: is rough	0.2647	0.2886	0.0239
102	aim: is for entertainment	0.2637	0.2963	0.0326
103	behaviour: can swim	0.2634	0.3082	0.0448
104	safety: is dangerous	0.2633	0.2905	0.0271
105	feeling: is pure	0.2631	0.2870	0.0239
106	function: can carry a small quantity (2264 1 ton) of goods	0.2612	0.2927	0.0315
107	shape: is ellipsoidal	0.2600	0.2837	0.0237
108	habit: can milk	0.2590	0.3070	0.0480
109	feeling: is elegant	0.2583	0.2848	0.0265
110	diet: eats seeds	0.2567	0.3023	0.0455
111	parts: has four wheels	0.2570	0.3004	0.0434
112	material: is made of glass	0.2569	0.2844	0.0275
113	parts: has a motor	0.2566	0.2855	0.0289
114	limb: has four legs	0.2559	0.3055	0.0496
115	feeling: is simple	0.2557	0.2800	0.0243
116	appearance: is smooth	0.2547	0.2869	0.0321
117	feeling: is cute	0.2453	0.2703	0.0249
118	limb: has short legs	0.2427	0.2803	0.0376
119	shape: is flat	0.2418	0.2648	0.0230
120	color: is black	0.2416	0.2691	0.0276
121	tail: has a long tail	0.2397	0.2726	0.0328
122	aim: is for family	0.2384	0.2685	0.0301
123	parts: has an audio	0.2378	0.2608	0.0229
124	existence: is fixed	0.2351	0.2539	0.0189
125	sound: is noisy	0.2330	0.2567	0.0237
126	diet: eats nectar	0.2277	0.2575	0.0298
127	diet: eats insects	0.2250	0.2564	0.0314
128	color: is white	0.2250	0.2504	0.0253
129	color: is gray	0.2238	0.2568	0.0330
130	usage mode: is handheld	0.2235	0.2412	0.0177
131	function: can transmit signal	0.2227	0.2447	0.0220
132	behaviour: can jump	0.2219	0.2573	0.0354
133	color: is gray	0.2219	0.2429	0.0210
134	parts: has a fan	0.2207	0.2442	0.0234
135	outside color: is cyan	0.2201	0.2360	0.0159
136	aim: is for engineering	0.2193	0.2436	0.0243
137	appearance: is furry	0.2178	0.2537	0.0360

Continued on next page

Table 9 – continued from previous page

Rank	Concept	Score	Relevance	Redundancy
138	feeling: is easy to be messy	0.2164	0.2344	0.0180
139	function: can give out sound	0.2164	0.2362	0.0198
140	habit: is strong	0.2161	0.2457	0.0296
141	current state: has been processed	0.2131	0.2295	0.0163
142	color: is white	0.2098	0.2268	0.0170
143	habit: is smart	0.2080	0.2375	0.0294
144	medicinal property: is mild	0.2075	0.2204	0.0129
145	parts: has a battery	0.2059	0.2226	0.0167
146	paws: has pads	0.2054	0.2400	0.0346
147	size: is big (compared to apples)	0.2045	0.2187	0.0142
148	tail: has a short tail	0.2043	0.2308	0.0265
149	limb: has long legs	0.2039	0.2295	0.0256
150	aim: is for military	0.2014	0.2174	0.0161
151	function: can show characters	0.2002	0.2194	0.0192
152	color: is black	0.1982	0.2183	0.0200
153	aim: is for safety	0.1981	0.2146	0.0164
154	function: can carry a larger number (> 10) of passengers	0.1978	0.2142	0.0164
155	power: consumes special fuel	0.1973	0.2126	0.0154
156	appearance: is hairless	0.1965	0.2085	0.0120
157	habit: is the predator	0.1952	0.2133	0.0181
158	habit: is noisy	0.1945	0.2170	0.0225
159	size: is small (compared to a mobile phone)	0.1904	0.2022	0.0118
160	aim: is for communication	0.1899	0.2065	0.0166
161	diet: eats fish	0.1897	0.2085	0.0188
162	marking: has patches	0.1891	0.2127	0.0236
163	power: is a high-power (>100 w) device	0.1888	0.2039	0.0152
164	current state: is shredded	0.1834	0.1971	0.0136
165	shape: is cubic	0.1830	0.1984	0.0153
166	appearance: has whiskers	0.1831	0.2084	0.0254
167	color: is golden	0.1790	0.1927	0.0137
168	habit: lives in solitary	0.1779	0.1958	0.0178
169	aim: is for rescue	0.1752	0.1912	0.0160
170	speed: moves slowly	0.1750	0.1849	0.0099
171	function: can storage data	0.1746	0.1872	0.0126
172	fitness: fits people with a hat	0.1747	0.1868	0.0122
173	size: is big (compared to pigs)	0.1731	0.1921	0.0190
174	function: can fly	0.1728	0.1847	0.0119
175	wing: has long wings	0.1727	0.1886	0.0159
176	usage scenarios: can be used in the sky	0.1718	0.1847	0.0128
177	behaviour: can climb trees	0.1716	0.1917	0.0201
178	habit: is cold-blooded	0.1705	0.1804	0.0099
179	parts: has only one usb interface	0.1693	0.1793	0.0100
180	habitat: is endangered	0.1670	0.1845	0.0176
181	power: consumes gasoline	0.1660	0.1800	0.0140
182	parts: has a propeller	0.1659	0.1776	0.0117
183	teeth: has buck teeth	0.1620	0.1844	0.0224
184	outside color: is green	0.1616	0.1703	0.0087
185	size: is middle (compared to apples)	0.1609	0.1704	0.0095
186	epidermis: has crust	0.1596	0.1671	0.0076
187	feeling: is gorgeous	0.1588	0.1669	0.0081
188	behaviour: can fly	0.1577	0.1713	0.0136
189	habitat: is domestic	0.1570	0.1726	0.0157
190	habit: moves slow	0.1562	0.1664	0.0101
191	parts: has volume control buttons	0.1556	0.1670	0.0114
192	growth: grows on the ground	0.1550	0.1630	0.0080

Continued on next page

Table 9 – continued from previous page

Rank	Concept	Score	Relevance	Redundancy
193	parts: has three wheels	0.1549	0.1659	0.0110
194	color: is brown	0.1542	0.1713	0.0171
195	marking: has spots	0.1540	0.1620	0.0080
196	parts: has a small screen (226410 inches)	0.1533	0.1640	0.0107
197	size: is middle (compared to cars)	0.1528	0.1650	0.0122
198	appearance: has tough skin	0.1489	0.1590	0.0101
199	outside color: is white	0.1489	0.1569	0.0080
200	parts: has armors	0.1472	0.1578	0.0106
201	parts: has a headphone jack	0.1451	0.1551	0.0100
202	feeling: is cool	0.1442	0.1509	0.0068
203	parts: has a cable	0.1418	0.1497	0.0079
204	function: can communicate in a short distance	0.1417	0.1525	0.0107
205	marking: has stripes	0.1403	0.1515	0.0112
206	feeling: is mature	0.1397	0.1461	0.0064
207	habitat: lives in the plains	0.1395	0.1529	0.0134
208	function: can play music	0.1381	0.1482	0.0101
209	habit: can hibernate	0.1375	0.1464	0.0089
210	function: can play videos	0.1371	0.1473	0.0102
211	appearance: has feathers	0.1346	0.1476	0.0131
212	limb: has two legs	0.1339	0.1476	0.0137
213	beak: has a short beak	0.1333	0.1476	0.0143
214	limb: is bipedal	0.1326	0.1476	0.0150
215	habit: is fierce	0.1326	0.1446	0.0120
216	parts: has more than four wheels	0.1321	0.1407	0.0086
217	epidermis: is hairy	0.1301	0.1360	0.0059
218	limb: has two arms	0.1289	0.1413	0.0124
219	behaviour: can lay eggs	0.1285	0.1409	0.0123
220	function: can float	0.1282	0.1359	0.0077
221	function: can heat	0.1277	0.1349	0.0072
222	usage scenarios: can be used in the sea	0.1277	0.1359	0.0082
223	habitat: lives in mountains	0.1271	0.1364	0.0093
224	habitat: lives in the forest	0.1264	0.1363	0.0099
225	parts: has weapons	0.1254	0.1335	0.0082
226	taste: tastes bitter	0.1211	0.1268	0.0057
227	habitat: lives in water	0.1211	0.1267	0.0055
228	habit: lives in nests	0.1206	0.1320	0.0114
229	outside color: is orange	0.1205	0.1259	0.0054
230	outside color: is violet	0.1193	0.1245	0.0051
231	fitness: fits people with moustache	0.1193	0.1235	0.0041
232	size: is small (compared to cars)	0.1185	0.1238	0.0053
233	habitat: lives in the jungle	0.1183	0.1280	0.0097
234	beak: has a needle beak	0.1176	0.1308	0.0132
235	parts: has only one network interface	0.1161	0.1233	0.0072
236	diet: eats plankton	0.1144	0.1200	0.0055
237	color: is yellow	0.1140	0.1242	0.0101
238	color: is brown	0.1119	0.1166	0.0048
239	usage scenarios: can be used in the river	0.1114	0.1182	0.0068
240	behaviour: can fish	0.1105	0.1175	0.0070
241	fitness: fits people with beard	0.1095	0.1139	0.0044
242	power: consumes electricity	0.1092	0.1137	0.0045
243	aim: is for sports	0.0998	0.1042	0.0044
244	color: is white	0.0997	0.1071	0.0074
245	habitat: lives in trees	0.0996	0.1089	0.0093
246	marking: has patches	0.0985	0.1026	0.0041
247	size: is middle (compared to a mobile phone)	0.0980	0.1028	0.0048

Continued on next page

Table 9 – continued from previous page

Rank	Concept	Score	Relevance	Redundancy
248	parts: has a jet engine	0.0962	0.1017	0.0055
249	color: is black	0.0961	0.0998	0.0037
250	function: can communicate in a long distance	0.0960	0.1023	0.0063
251	outside color: is brown	0.0956	0.0985	0.0029
252	edibility: is rare	0.0952	0.0989	0.0037
253	usage scenarios: can be used in the lake	0.0927	0.0980	0.0053
254	parts: has a large screen (> 10 inches)	0.0903	0.0959	0.0056
255	habitat: lives in the ocean	0.0903	0.0943	0.0040
256	habitat: lives in the traveling	0.0889	0.0944	0.0055
257	color: is red	0.0872	0.0914	0.0042
258	function: can photograph	0.0864	0.0919	0.0055
259	feeling: is naive	0.0855	0.0886	0.0031
260	parts: has two wheels	0.0840	0.0877	0.0037
261	tail: has a colorful tail	0.0839	0.0887	0.0048
262	parts: has many usb interfaces	0.0838	0.0888	0.0050
263	safety: is dangerous	0.0836	0.0864	0.0028
264	parts: has a camera	0.0831	0.0885	0.0053
265	marking: has stripes	0.0827	0.0861	0.0035
266	taste: tastes puckery	0.0824	0.0851	0.0027
267	aim: is for cleaning	0.0808	0.0844	0.0036
268	epidermis: is angular	0.0775	0.0800	0.0025
269	outside color: is transparent	0.0769	0.0804	0.0035
270	epidermis: is barbed	0.0737	0.0764	0.0027
271	shape: is schistose	0.0731	0.0758	0.0027
272	neck: has a short neck	0.0731	0.0780	0.0049
273	outside color: is black	0.0730	0.0759	0.0029
274	marking: has spots	0.0727	0.0756	0.0029
275	color: is blue	0.0685	0.0718	0.0033
276	other body parts: has fins	0.0644	0.0681	0.0037
277	material: is made of cloth	0.0640	0.0664	0.0024
278	parts: has a track	0.0630	0.0654	0.0024
279	usage scenarios: can be used on the track	0.0628	0.0654	0.0027
280	current state: is shelled	0.0624	0.0645	0.0021
281	smell: is smelly	0.0621	0.0649	0.0028
282	paws: has hooves	0.0618	0.0657	0.0039
283	appearance: has shells	0.0618	0.0648	0.0030
284	function: can be located	0.0613	0.0654	0.0041
285	color: is yellow	0.0607	0.0639	0.0032
286	color: is transparent	0.0602	0.0630	0.0028
287	color: is green	0.0598	0.0626	0.0028
288	habit: is venomous	0.0597	0.0617	0.0020
289	parts: has many network interfaces	0.0577	0.0603	0.0026
290	limb: has tentacle	0.0570	0.0594	0.0024
291	shape: is cubic	0.0566	0.0591	0.0024
292	parts: has a mast	0.0558	0.0586	0.0028
293	parts: has a wrist band	0.0550	0.0567	0.0017
294	beak: has a curved beak	0.0531	0.0569	0.0038
295	function: can refrigerate	0.0530	0.0551	0.0022
296	habit: is nocturnal	0.0525	0.0558	0.0034
297	shape: is cylindrical	0.0511	0.0526	0.0015
298	other body parts: has a shell	0.0506	0.0532	0.0026
299	aim: is for cleaning	0.0506	0.0528	0.0022
300	shape: is ellipsoidal	0.0501	0.0518	0.0017
301	power: consumes wind power	0.0486	0.0502	0.0016
302	parts: has an antenna	0.0483	0.0503	0.0019

Continued on next page

Table 9 – continued from previous page

Rank	Concept	Score	Relevance	Redundancy
303	beak: has a hooked beak	0.0463	0.0498	0.0035
304	size: is middle (compared to pigs)	0.0429	0.0455	0.0025
305	horn: has short horns	0.0416	0.0439	0.0022
306	horn: has cuspidal horns	0.0415	0.0437	0.0022
307	parts: has a sunroof	0.0375	0.0389	0.0014
308	appearance: is mucous	0.0364	0.0378	0.0014
309	color: is brown	0.0358	0.0369	0.0010
310	color: is yellow	0.0357	0.0369	0.0012
311	shape: is star-shaped	0.0347	0.0358	0.0011
312	parts: has a touch pad	0.0344	0.0370	0.0026
313	material: is made of wood	0.0316	0.0329	0.0013
314	color: is red	0.0307	0.0319	0.0012
315	horn: has long horns	0.0303	0.0320	0.0017
316	function: can dive	0.0300	0.0313	0.0013
317	color: is green	0.0287	0.0305	0.0019
318	color: is green	0.0282	0.0291	0.0009
319	outside color: is blue	0.0276	0.0284	0.0008
320	outside color: is gray	0.0275	0.0284	0.0009
321	appearance: is acicular	0.0266	0.0280	0.0014
322	power: consumes manpower	0.0262	0.0271	0.0008
323	price: is cheap	0.0260	0.0269	0.0009
324	parts: has a sail	0.0255	0.0267	0.0012
325	teeth: has tusks	0.0169	0.0178	0.0009
326	wing: has short wings	0.0166	0.0172	0.0007
327	horn: has curved horns	0.0142	0.0150	0.0008
328	usage scenarios: can be used in the space	0.0127	0.0131	0.0004
329	habitat: lives in the cave	0.0107	0.0111	0.0004
330	habit: is the scavenger	0.0107	0.0111	0.0004
331	beak: has a long beak	0.0104	0.0109	0.0005
332	appearance: has scales	0.0064	0.0066	0.0002
333	color: is blue	0.0026	0.0028	0.0002
334	color: is red	0.0020	0.0021	0.0001
335	color: is orange	0.0015	0.0016	0.0001
336	current state: is peeled	0.0012	0.0013	0.0001
337	color: is orange	0.0012	0.0012	0.0001
338	color: is blue	0.0012	0.0012	0.0001
339	color: is brown	0.0011	0.0011	0.0001
340	color: is cyan	0.0007	0.0008	0.0000
341	color: is violet	0.0006	0.0007	0.0000
342	shape: is cubic	0.0006	0.0007	0.0000
343	habitat: lives in fields	0.0006	0.0007	0.0000
344	color: is violet	0.0005	0.0006	0.0000
345	usage mode: is head-mounted	0.0005	0.0006	0.0000
346	color: is cyan	0.0005	0.0005	0.0000
347	color: is orange	0.0005	0.0005	0.0000
348	color: is violet	0.0005	0.0005	0.0000
349	color: is cyan	0.0004	0.0004	0.0000
350	habitat: lives in the bush	0.0003	0.0003	0.0000
351	existence: is rare	0.0003	0.0003	0.0000
352	habitat: lives in the arctic	0.0002	0.0003	0.0000
353	horn: has only one horn	0.0002	0.0002	0.0000
354	shape: is globular	0.0001	0.0001	0.0000
355	beak: has a dagger beak	0.0000	0.0000	0.0000
356	smell: is smelly	0.0000	0.0000	0.0000
357	habitat: lives in coastal places	0.0000	0.0000	0.0000

Continued on next page

Table 9 – continued from previous page

Rank	Concept	Score	Relevance	Redundancy
358	habitat: lives in the desert	0.0000	0.0000	0.0000
359	taste: tastes spicy	0.0000	0.0000	0.0000